Talanta 79 (2009) 289–294

Contents lists available at ScienceDirect

Talanta

journal homepage: www.elsevier.com/locate/talanta

Electrochemical characterization of a superoxide biosensor based on the co-immobilization of cytochrome *c* and XOD on SAM-modified gold electrodes and application to garlic samples

Montserrat Cortina-Puig*, Xavier Muñoz-Berbel, Carole Calas-Blanchard, Jean-Louis Marty

IMAGES EA 4218, Université de Perpignan Via Domitia, 52 avenue Paul Alduy, 66860 Perpignan Cedex, France

ARTICLE INFO

Article history:
Received 19 December 2008
Received in revised form 17 March 2009
Accepted 23 March 2009
Available online 31 March 2009

Keywords:
Impedance spectroscopy
Amperometry
Cytochrome *c*-based biosensor
Antioxidant capacity
Screen-printed gold electrodes

ABSTRACT

This paper describes the characterization and optimization of an amperometric cytochrome *c* (cyt *c*)-based sensor for the determination of the antioxidant capacity of pure substances and natural samples. The cyt *c* and the xanthine oxidase (XOD) enzyme were co-immobilized on the electrode using the combination of several long-chain thiols. The self-assembled monolayer (SAM) was optimized in terms of composition and ratio between thiols. The immobilization protocol for both cyt *c* and XOD and the SAM formation time were evaluated through electrochemical methods, such as cyclic voltammetry (CV), square wave voltammetry (SWV), chronoamperometry (CA) and impedance spectroscopy (IS). Finally, the biosensor was applied to the determination of the antioxidant capacity of pure alliin and two compounds extracted from garlic bulbs.

1. Introduction

Reactive oxygen species (ROS) represent the most important free radicals generated in living systems, especially the superoxide ($O_2^{\bullet -}$), the peroxyl (ROO$^\bullet$), the alkoxyl (RO$^\bullet$) or the hydroxyl (OH$^\bullet$) radicals. ROS, naturally generated during the metabolism, can damage biological structures such as proteins, lipids or DNA [1]. This oxidative damage is thought to play a causative role in aging [2,3] and several degenerative diseases associated with it, such as heart disease [4,5], cataracts [6,7], cognitive dysfunction [8,9] and cancer [10,11]. Antioxidants, which quench reactive free radicals, can prevent the oxidation of other molecules and thus they can have health-promoting effects in the prevention of degenerative diseases [12]. The interest in antioxidants is increasing because of their high capacity in scavenging free radicals related to various diseases [13].

Traditionally, antioxidants have been detected using chromatographic, spectrophotometric or fluorescence approaches [14]. Lately, electrochemical biosensors have become promising tools since they provide the advantage of rapid and real-time analysis, which increase the assay speed, flexibility, low cost and favour the development of automated and multi-target systems [15]. Electrochemical methods based on biosensors are particularly suitable for the sensitive determination of the $O_2^{\bullet -}$ radical at real-time. These methods have been classically based on either superoxide dismutase (SOD) or cytochrome *c* (cyt *c*).

The first one is based on the specific dismutation of the $O_2^{\bullet -}$ radical by SOD to produce hydrogen peroxide (H_2O_2), followed by the detection of electrooxidation of H_2O_2 at the electrode surface [16,17]. However, the oxidation potential of H_2O_2 is very high (>0.5 V vs. Ag/AgCl), hence resulting in interference problems that limit their practical application.

The second group is based on the reduction of cyt *c* immobilized on gold electrodes by the $O_2^{\bullet -}$ radical and the following reoxidation of the protein at the electrode surface. Commonly, the $O_2^{\bullet -}$ radical is enzymatically produced in solution using the xanthine oxidase (XOD)/hypoxanthine (HX) system. Thus, the obtained oxidation current is proportional to the $O_2^{\bullet -}$ concentration [18]. Usually, the electron transfer between the electrode and the redox protein is extremely slow. Consequently, traditional electrochemical methods cannot detect it [19]. An elegant way to modify gold electrodes, the most commonly used in this area, is the formation of self-assembled monolayers (SAMs). Long-chain alkanethiols show a high efficiency of communication between cyt *c* and the electrode [20–22]. However, these sensors usually show very small signal responses due to spontaneous dismutation of the $O_2^{\bullet -}$ radical in the way from the bulk, where it is generated as previously detailed, to the electrode surface where reacts with the cyt *c*.

This paper describes the characterization and application of a superoxide biosensor based on the co-immobilization of cyt *c* and

* Corresponding author. Tel.: +33 468662253; fax: +33 468662223.
E-mail address: mcortina12@gmail.com (M. Cortina-Puig).

0039-9140/$ – see front matter © 2009 Elsevier B.V. All rights reserved.
doi:10.1016/j.talanta.2009.03.046

XOD on SAM-modified gold electrodes. The composition of the SAM, the time formation and the process of immobilization of the cyt *c* and XOD on the SAM-modified electrodes were optimized according to the intensity of the cyt *c* oxidation peak and the activity of the XOD enzyme. The developed biosensor was then applied to the determination of the antioxidant capacity of pure alliin and two compounds extracted from garlic bulbs.

2. Materials and methods

2.1. Reagents and chemicals

XOD from buttermilk (EC 1.17.3.2), catalase from bovine liver (EC 1.11.1.6), cyt *c* from horse heart and HX, 1-ethyl-3-(3-dimethylaminopropyl)carbodiimide (EDC), 11-mercapto-1-undecanol (MU), 11-mercaptoundecanoic acid (MUA), 3,3′-dithiodipropionic acid (DTDPA), potassium hexacyanoferrate (III), potassium hexacyanoferrate (II) trihydrate, uric acid and 30% H_2O_2 were purchased from Sigma (St. Quentin Fallavier, France). N-hydroxysuccinimide (NHS) and pure alliin were provided by Fluka (France). All reagents were of analytical grade and were used without further purification. All solutions were prepared using Milli-Q water.

Both alliin and allicin extracted from garlic bulbs were kindly provided by Dr. E. Touloupakis from the University of Crete. Alliin solutions were prepared in 50 mM sodium phosphate buffer (Na-PBS) pH 6.5 while allicin was diluted in 96% ethanol (Carlo Erba, Italy).

2.2. Electrochemical measurements

Electrochemical measurements were carried out using an AUTOLAB PGSTAT12 Potentiostat (Eco Chemie, BV, The Netherlands) containing a FRA-2 module. Cyclic voltammetry (CV) and square wave voltammetry (SWV) measurements were recorded between −0.15 and 0.25 V at a scan rate of 100 mV s^{-1}. Chronoamperometric (CA) data were obtained by applying 150 mV for 15 s. Impedance spectroscopy (IS) spectra were recorded at the open circuit potential (0.25 ± 0.05 vs. Ag/AgCl) over a frequency range from 50 kHz to 0.1 Hz, using a sinusoidal AC potential perturbation of 5 mV. The measurement time was around 8 min after registering 18 points per frequency decade. All measurements given in this work are in relation to the Ag/AgCl reference electrode.

Amperometric measurements for the determination of the scavenging capacity of several antioxidants were made using a 641VA potentiostat (Metrohm, Switzerland), connected to a BD40 (Kipp & Zonen, The Netherlands) *X–t* recorder at 150 mV. Assays were performed in triplicate with three different electrodes.

2.3. Electrode pre-treatment and preparation

Gold screen-printed electrodes (DropSens, Spain) of 12.6 mm^2 were used as working electrodes. A platinum wire and a double-junction Ag/AgCl electrode (Thermo Orion 900200) were used as counter and reference electrodes.

Electrodes were electrochemically cleaned by cycling the potential between 0 and +1.4 V at the scan rate of 100 mV s^{-1} in 0.1 M H_2SO_4 until the characteristic cyclic voltammogram for a clean gold electrode was obtained. After this, electrodes were rinsed with water and ethanol and incubated in the ethanolic solution containing the thiols. The modified gold surface was then rinsed thoroughly with absolute ethanol and with water to remove any unattached thiol molecules. Cyt *c* and XOD were then immobilized on the modified electrode surface. Regarding the literature, four different procedures for their immobilization were tested, based on direct adsorption or on covalent attachment.

Protocol 1: Electrodes were incubated in a 50 μM cyt *c* + 50 mU mL^{-1} XOD solution, prepared in 5 mM K-PBS pH 7.0, for 2 h [23].

Protocol 2: Electrodes were first incubated in a 50 μM cyt *c* + 50 mU mL^{-1} XOD solution in buffer for 2 h. After washing with the buffer solution, electrodes were incubated in an aqueous solution of 5 mM EDC for 30 min [24].

Protocol 3: Electrodes were also incubated in a 50 μM cyt *c* + 50 mU mL^{-1} XOD solution in buffer. After 2 h, and without a cleaning step, EDC was added to obtain a concentration of 5 mM, and electrodes were incubated with the solution for 30 min [25].

Protocol 4: Electrodes were first incubated in an aqueous solution of 200 mM EDC and 50 mM NHS for 30 min. The excess of EDC and NHS was eliminated by cleaning with buffer. Finally, electrodes were incubated in a 50 μM cyt *c* + 50 mU mL^{-1} XOD solution in buffer for 30 min [20].

Lastly, the cyt *c*/XOD-modified electrodes were rinsed again with the same buffer solution to remove non-attached substances.

Fresh electrodes were prepared before each experiment.

2.4. Measurement of the superoxide scavenging capacity

The detection principle was based on the redox reaction between the cyt *c* and the $O_2^{\bullet -}$ radical generated by the HX/XOD system. The immobilized cyt *c* was reduced by $O_2^{\bullet -}$ and immediately regenerated at the electrode surface polarized at its oxidation potential (150 mV vs. Ag/AgCl). The generated oxidation current was proportional to the superoxide concentration in solution. The addition of antioxidants reduced the radical concentration and thus the oxidation current, allowing the quantification of the antioxidant capacity.

All amperometric experiments were carried out under constant stirring in 0.1 M Na-PBS with 100 μM EDTA pH 7.5. Before measurements, a catalase solution (final concentration in the cell = 10 U mL^{-1}) was added to avoid interferences from the H_2O_2, generated as a final product of the enzymatic reaction or by the spontaneous dismutation of $O_2^{\bullet -}$. Once the stable baseline was established, the HX solution was added into the cell (final concentration = 80 μM) and a steady-state superoxide level was recorded corresponding to the maximum response. Stock solutions of HX were prepared in 50 mM K-PBS pH 7.5 with 0.01 M KCl and 0.5 mM EDTA.

In the investigation of the role of superoxide scavengers, aliquots of the antioxidant samples were added and the current decrease was recorded after the addition of 80 μM HX. The decrease of the signal was normalized regarding the initial ROS signal, which minimized the sensitivity variation between sensors. This initial ROS signal was recorded before each addition of antioxidant in order to obtain more precise differential measurements. The antioxidant capacity was calculated by considering the sample concentration necessary for 50% signal inhibition (IC_{50}). This value was used for comparison between antioxidants: low IC_{50} corresponded to a high antioxidant capacity.

The direct influence of all tested samples on the CV of cyt *c* was investigated before the determination of their antioxidant capacity.

3. Results and discussion

3.1. Optimization of the SAM composition

Electrodes were prepared as detailed in Section 2.3 (*protocol* 4) using several compositions and ratios of thiols selected from the literature. In terms of composition, 10 mM MUA (10-MUA) [24], 5 mM MU and 5 mM MUA (5-MU/5-MUA) [20], 3.75 mM MU and 1.25 mM MUA (3.75-MU/1.25-MUA) [26] and 5 mM MU, 5 mM MUA and 5 mM DTDPA (5-MU/5-MUA/5-DTDPA) [27] were chosen. Table 1

Table 1
Magnitude of the oxidation peak current for the cyt *c* when using different compositions and ratios of thiols samples. CV was performed in 5 mM K-PBS pH 7.0. Standard deviations are given from three electrodes.

SAM composition	I (μA)
10-MUA	0.048 ± 0.006
5-MU/5-MUA	0.102 ± 0.006
3.75-MU/1.25-MUA	0.125 ± 0.005
5-MU/5-MUA/5-DTDPA	0.107 ± 0.007

shows the magnitude of the oxidation peak for the cyt *c* when using the thiols samples previously described.

The 3.75-MU/1.25-MUA mixture was found to give the highest peak intensity and thus, this composition was used in the following assays.

3.2. Optimization of the cyt c and XOD immobilization process

As detailed in Section 2.3, four different procedures for the immobilization of the cyt *c* and the XOD were tested, based on direct adsorption or on covalent attachment. Table 2 shows the current response of the anodic peak of the cyt *c* depending on the protocol of immobilization.

The highest current response was obtained when using the *protocol* 1. However, this sensor showed low stability and a huge reduction of the signal was recorded after 10 min. On the other hand, sensors prepared following the *protocol* 4 showed high signal responses and long stability with time. Further, by co-immobilizing cyt *c* and XOD through this protocol, amperometric signal responses were found to be almost 15 times bigger than those reported in the bibliography [21,22]. As cyt *c* and XOD were very close, generated $O_2^{\bullet -}$ radicals could quickly react with cyt *c*, avoiding its spontaneous dismutation. From this point, all the electrodes of this work were prepared by following the *protocol* 4.

3.3. Optimization of the SAM formation time

Biosensors preparation was made as detailed in Section 2.3. The SAM formation process was monitored using IS as described in Section 2.2 by following the isolating properties of the SAM. Fig. 1a shows the impedance spectra of bare and SAM-modified electrodes in $Fe(CN)_6^{3-/4-}$ after different exposure times to the thiols solution (from 1 to 168 h of exposure). IS spectra were fitted to the equivalent circuit shown inset and the magnitude of the charge transfer resistance, R_{CT}, obtained from the fitting was plotted in Fig. 1b.

The R_{CT} value was found to increase with the exposition time to the thiols solution until 96 h, when a relative constant value was obtained. This suggested that the adsorption and rearrangement of thiols on the electrode surface to build a SAM impeded ferrocyanide molecules to flow and exchange electrons with the gold. 96 h may be the time required for the thiols to completely cover the electrode surface.

SWV and CA data were respectively used to determine the amount of cyt *c* and the activity of the XOD immobilized on the electrode surface with the exposition time. These measurements

Table 2
Variation of the oxidation peak current for the cyt *c* with time, depending on the protocol of immobilization. CV was performed in 5 mM K-PBS pH 7.0.

Protocol of immobilization	I (μA) (t = 0 min)	I (μA) (t = 10 min)	% Signal decrease
Protocol 1	0.250	0.124	50.3
Protocol 2	0.091	0.078	13.9
Protocol 3	0.063	0.053	15.5
Protocol 4	0.126	0.125	0.1

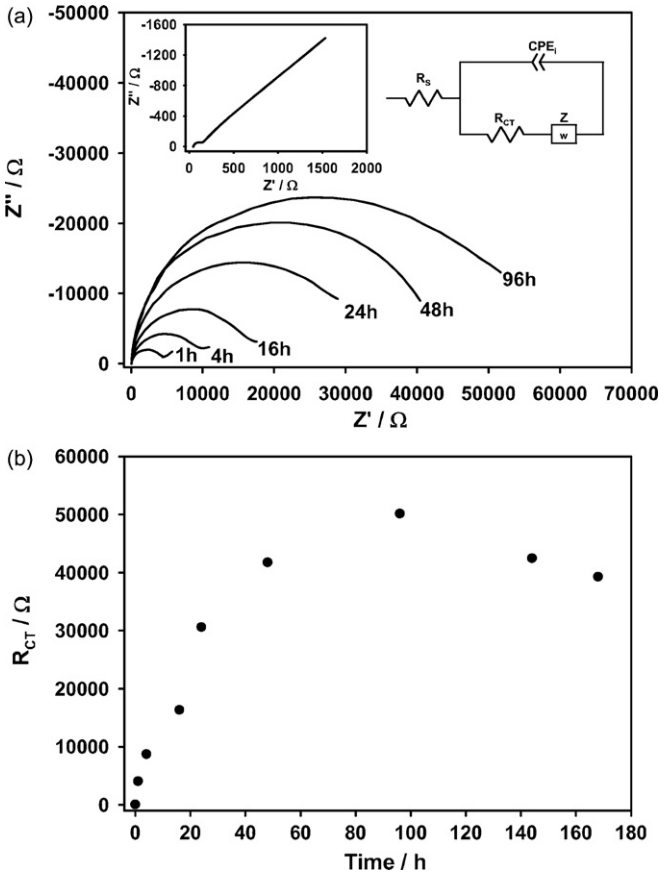

Fig. 1. (a) Complex plane plot of the gold screen-printed electrodes in 1 mM $Fe(CN)_6^{3-/4-}$ with the incubation time. The impedance plot of a bare gold electrode and the equivalent circuit used in the fitting of the data are shown in the inset. The circuit contains the solution resistance (R_S), the charge-transfer resistance (R_{CT}), the Warburg's impedance (Z_W) and the interface constant phase element (CPE_i). (b) Representation of the variation of the R_{CT} magnitude (after fitting with the equivalent circuit here exposed) with the incubation time.

were made by following the protocols detailed in Section 2.2. Fig. 2a shows the SWV response peak of cyt *c* covalently immobilized on the electrode after different times of incubation. The intensity of the cyt *c* peak with the incubation time is represented inset.

The cyt *c* peak current increased with the exposition time until 96 h, when it reached a plateau. Thus, the maximum amount of cyt *c* immobilized was obtained after at least 96 h of exposition. No redox wave was observed at the bare electrode (data not shown).

On the other hand, Fig. 2b shows the current response of the XOD enzyme after several incubation times. In this case, the maximum response of the enzyme was also found after 96 h of incubation of the sensor in the thiols solution. Thus, all the sensors used in this work were incubated at least 96 h in the thiols solution.

3.4. Electrochemical characterization of immobilized cyt c

The electrochemical properties of the immobilized cyt *c* were evaluated using CV as described in Section 2.2 but modifying the scan rate from 20 to 100 mV s^{-1}. Characteristic cyclic voltammograms for cyt *c* immobilized on a mixed SAM are shown in Fig. 3a. A pair of well-defined redox peaks were observed with a formal potential, $E^{o\prime}$ taken as $(E_p^c + E_p^a)/2$, of 62 mV and with a peak-to-peak separation value, ΔE_p, of 41 mV, at a scan rate of 100 mV s^{-1}. As can be seen, the peak-to-peak separation remained constant with the increase of the scan rate, and both the anodic and cathodic peak currents were linear with the scan rates (the inset of Fig. 3a), indicating a typical adsorption-controlled electrode.

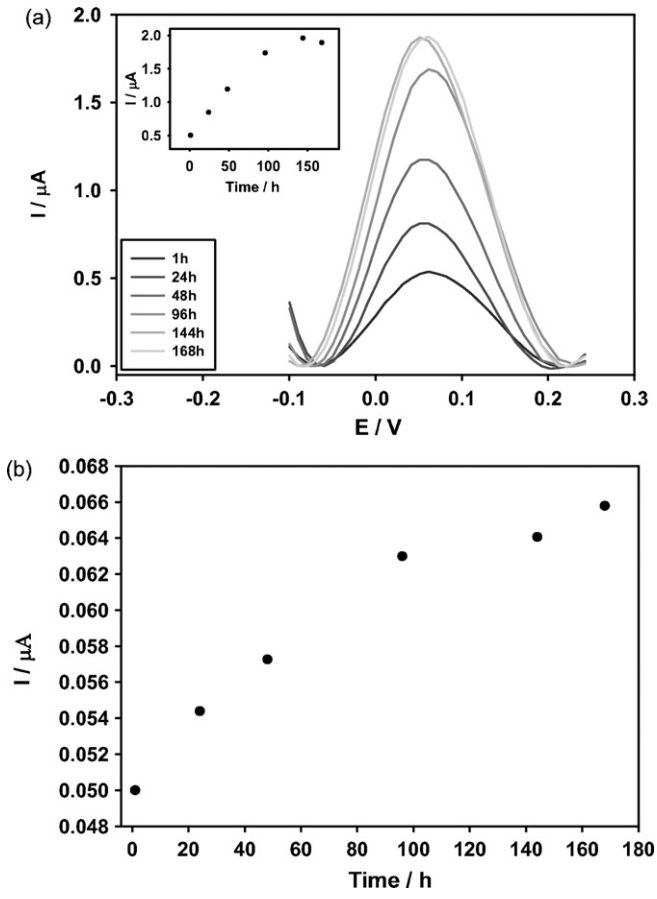

Fig. 2. (a) Representation of the current response of the cyt *c* covalently immobilized on electrodes modified after different times of incubation in the thiols solution. Measurements were performed in 5 mM K-PBS pH 7.0. The dependence of the peak current on the incubation time is shown inset. (b) Representation of the current response corresponding to the XOD activity with the incubation time in the thiols solution. Current values were obtained from CA in 5 mM K-PBS pH 7.0 containing 80 μM HX.

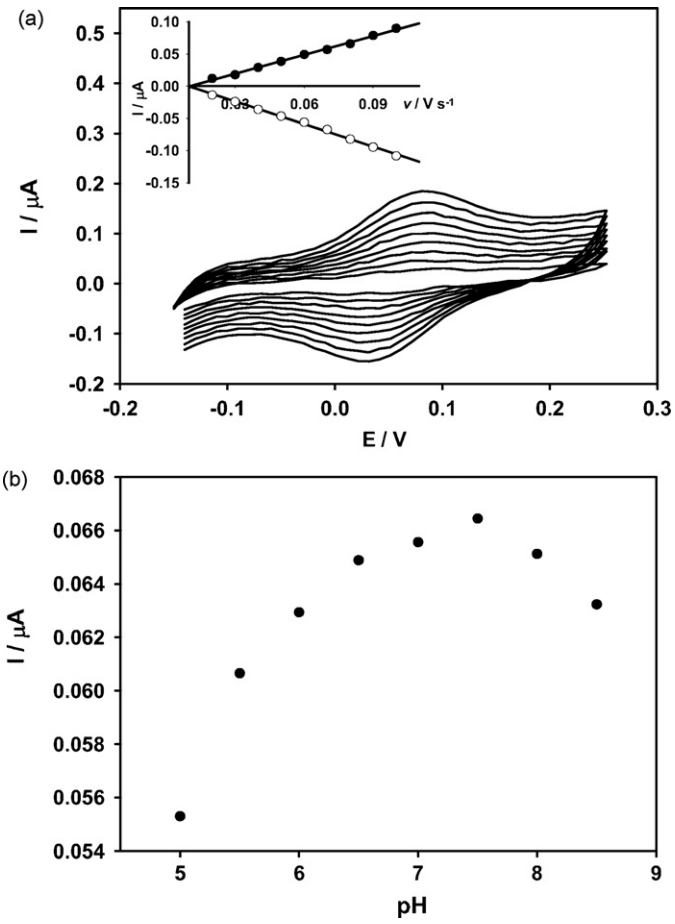

Fig. 3. (a) Cyclic voltammograms of the cyt *c* immobilized on the electrode at different scan rates (from inner to outer): 20, 30, 40, 50, 60, 70, 80, 90 and 100 mV s^{-1} in 5 mM K-PBS pH 7.0 at room temperature. Inset: the cathodic and anodic peak currents are plotted versus the scan rate (ν). (b) Representation of the dependence of the steady-state cathodic peak current on the pH. Cyclic voltammetry was performed in 5 mM K-PBS.

According to Laviron's equation [28]:

$$I_p = \frac{n^2F^2A\Gamma\nu}{4RT} = \frac{nFQ\nu}{4RT} \quad (1)$$

where I_p is the peak current of the anodic or cathodic peaks, Γ is the surface coverage of the electroactive substance (mol cm^{-2}), A is the electrode area (cm^2), Q is the quantity of charge (C), calculated from the peak area of the voltammograms, n is the number of electrons transferred. F, R, T and ν have their usual meanings. From the slope of the I_p–ν curve, n was calculated to be 1.1. Therefore, the redox of cyt *c* on a SAM-modified gold electrode is a single electron transfer reaction. The average surface coverage (Γ) of the immobilized cyt *c* was calculated to be 14.5 pmol cm^{-2}. This value was very close to the theoretical monolayer coverage, 14.3 pmol cm^{-2}, which was estimated using the crystallographic dimensions of cyt *c* (3.0 mm × 3.4 mm × 3.4 mm), and assuming one molecule with the long axis parallel to the electrode surface (3.4 mm × 3.4 mm) [29].

The small peak-to-peak separation value illustrates a fast electron transfer rate. The electron transfer rate constant, k_S, was estimated to be 42.8 s^{-1} using the following equation:

$$m = \frac{RTk_S}{Fn\nu} \quad (2)$$

when $n\Delta E_p < 200$ mV [28], where m is a parameter related to the peak-to-peak separation. F, R, T, n and ν have their usual meanings.

On the other hand, the effect of pH was investigated from 5.0 to 8.5. Fig. 3b shows the change of cathodic peak intensity with pH. As can be seen, the maximum response appeared at pH 7.5. Thus, to obtain the maximum sensitivity and bioactivity, a buffer of pH 7.5 was used throughout the research.

3.5. Optimization of the HX concentration

In the optimization of the HX concentration, CA measurements were carried out as described in Section 2.2 using eight solutions, ranging from 0 to 140 μM HX. The current response of the sensor with the concentration of HX was plotted (Fig. 4). As can be seen, the current response increased from 0 to 80 μM, when it stabilized and thus, 80 μM HX was chosen as the optimal concentration for the development of the scavenging biosensor.

3.6. Response of the biosensor to potential interferences

The influence of H_2O_2 and uric acid, the final products of the enzymatic $O_2^{\bullet-}$-generation system, was also investigated. An externally added H_2O_2 concentration of 480 μM (six times HX concentration) showed an influence on the $O_2^{\bullet-}$ signal of about 4%. Furthermore, the sensor gave no response to the same externally added uric acid concentration.

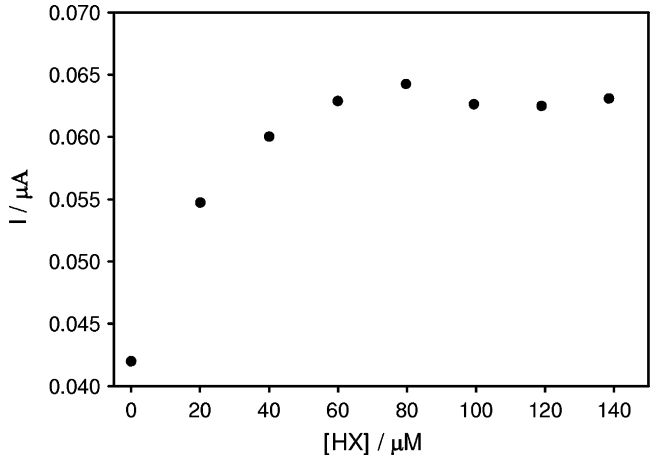

Fig. 4. Dependence of the CA oxidation current on the HX concentration using the cyt *c*/XOD-modified electrodes. Current values were obtained in 0.1 M Na-PBS with 100 μM EDTA pH 7.5.

3.7. Application of the superoxide radical sensor to the detection of the antioxidant capacity of pure substances and real samples of garlic

The developed biosensor was then applied to the determination of the antioxidant capacity of *Allium* species, particularly pure alliin and both natural alliin and allicin extracted from garlic bulbs. It has been previously reported that organosulfur compounds from garlic inhibit the peroxidation of lipids and possess antioxidant and radical scavenging activity [30].

In this case, amperometric measurements were made by following the protocols detailed in Sections 2.2 and 2.4. In Fig. 5 the current decrease versus the alliin concentration is shown.

The hyperbolic fit of alliin extracted from garlic bulbs allowed the determination of IC_{50}. Such behaviour corresponds to the empirical Hill equation, which can describe a variety of sensor responses [31]:

$$y = \frac{Bx}{C + x} \quad (3)$$

where y and x respectively correspond to the percentage of signal inhibition and the antioxidant concentration in solution, and B and C are constant values. Thus, the IC_{50} of the alliin extracted from garlic bulbs was calculated to be $100 \pm 8\ \mu g\ mL^{-1}$.

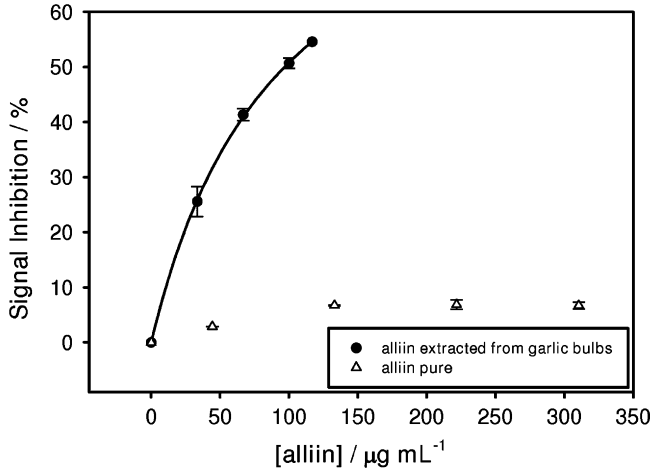

Fig. 5. Representation of the signal inhibition with the concentration of pure alliin and alliin extracted from garlic bulbs. Superoxide generated with 80 μM HX. Error bars are deduced from three repeated measurements.

However, pure alliin showed a poor antioxidant capacity. This fact agrees with other studies showing its weak antioxidative activity [32]. Therefore, the antioxidant capacity of the alliin extracted from garlic bulbs may be attributed to the presence of other antioxidant substances generated during the extraction process.

On the other hand, allicin extracted from garlic bulbs was found to have prooxidant properties (data not shown). Although allicin is thought to be the principal bioactive compound present in garlic extracts, some of its properties make it difficult to be used in practice: it is chemically unstable at room temperature and readily decomposes to other species, which may reduce its antioxidant activity or even enhance prooxidant activity [33].

The direct influence of the alliin extracted from garlic bulbs on the CV of cyt *c* was investigated. CV and SWV measurements were performed in buffer and in a 161 $\mu g\ mL^{-1}$ alliin solution. The influence of this antioxidant on cyt *c* peak currents was less than 1%. Furthermore, the mixed SAM showed effective blocking for the tested antioxidants and no faradaic responses were observed.

4. Conclusions

In this paper, an enzymatic biosensor based on the co-immobilization of cyt *c* and XOD was developed for the detection of the antioxidant capacity of pure substances and garlic extracts. The composition and ratio between thiols and the protocol to co-immobilize the cyt *c* and the XOD were optimized to supply high current signals. The 3.75-MU/1.25-MUA mixture and the *protocol* 4, where the cyt *c* and the XOD were immobilized on the previously activated mixed SAM, were found to be the optimal conditions. In terms of incubation time, after 96 h of incubation the amount of cyt *c* and the XOD activity reached a maximum and thus, this time was chosen as the minimum time necessary for the correct reorganization of the thiols. This biosensor was applied to the detection of the antioxidant capacity of pure alliin and alliin and allicin extracted from garlic bulbs. Alliin extracted from garlic bulbs showed better antioxidant capacity than the pure one, probably for the presence of other antioxidants in the sample which enhanced their effect.

Acknowledgment

The authors greatly acknowledge the European Commission for financial support through the project "Nutra-Snacks" (FOOD-CT-2005-023044).

References

[1] H.E. Seifried, D.E. Anderson, E.I. Fisher, J.A. Milner, J. Nutr. Biochem. 18 (2007) 567.
[2] K.B. Choksi, J. Papaconstantinou, Free Radic. Biol. Med. 44 (2008) 1795.
[3] M.Y.B. Çimen, Clin. Chim. Acta 390 (2008) 1.
[4] S.K. Wattanapitayakul, J.A. Bauer, Pharmacol. Ther. 89 (2001) 187.
[5] B.Z. Simkhovich, M.T. Kleinman, R.A. Kloner, J. Am. Coll. Cardiol. 52 (2008) 719.
[6] V.N. Reddy, E. Kasahara, M. Hiraoka, L.R. Lin, Y.S. Ho, Exp. Eye Res. 79 (2004) 859.
[7] M.A. Marchetti, W. Lee, T.L. Cowell, T.M. Wells, H. Weissbach, M. Kantorow, Exp. Eye Res. 83 (2006) 1281.
[8] V. Valcour, B. Shiramizu, Mitochondrion 4 (2004) 119.
[9] X. Zhu, M.A. Smith, K. Honda, G. Aliev, P.I. Moreira, A. Nunomura, G. Casadesus, P.L.R. Harris, S.L. Siedlak, G. Perry, J. Neurol. Sci. 257 (2007) 240.
[10] W. Yan, W. Chen, L. Huang, J. Contr. Release 130 (2008) 22.
[11] A. Roessner, D. Kuester, P. Malfertheiner, R. Schneider-Stock, Pathol. Res. Pract. 204 (2008) 511.
[12] H. Basu, A. Vecchio, F. Flider, F. Orthoeter, J. Am. Oil Chem. Soc. 78 (2001) 665.
[13] E.M. Silva, J.N.S. Souza, H. Rogez, J.F. Rees, Y. Larondelle, Food Chem. 101 (2007) 1012.
[14] L.M. Magalhães, M.A. Segundo, S. Reis, J.L.F.C. Lima, Anal. Chim. Acta 613 (2008) 1.
[15] B. Prieto-Simón, M. Cortina, M. Campàs, C. Calas-Blanchard, Sens. Actuators B 129 (2008) 459.
[16] L. Campanella, G. Favero, L. Persi, M. Tomassetti, J. Pharm. Biomed. Anal. 23 (2000) 69.
[17] Y. Tian, L. Mao, T. Okajima, T. Ohsaka, Anal. Chem. 74 (2002) 2428.

[18] K. Tammeveski, T.T. Tenno, A.A. Mashirin, E.W. Hillhouse, P. Manning, C.J. McNeil, Free Radic. Biol. Med. 25 (1998) 973.
[19] H.A.O. Hill, G.A. Lawrance, J. Electroanal. Chem. 270 (1989) 309.
[20] B. Ge, F. Lisdat, Anal. Chim. Acta 454 (2002) 53.
[21] S. Ignatov, D. Shishniashvili, B. Ge, F.W. Scheller, F. Lisdat, Biosens. Bioelectron. 17 (2002) 191.
[22] F. Lisdat, B. Ge, E. Ehrentreich-Forster, R. Reszka, F.W. Scheller, Anal. Chem. 71 (1999) 1359.
[23] R.A. Clark, E.F. Bowden, Langmuir 13 (1997) 559.
[24] K.B. Holt, Langmuir 22 (2006) 4298.
[25] M.K. Beissenhirtz, R.C.H. Kwan, K.M. Ko, R. Renneberg, F.W. Scheller, F. Lisdat, Phytother. Res. 18 (2004) 149.
[26] A.V. Krylov, M. Beissenhirtz, H. Adamzig, F.W. Scheller, F. Lisdat, Anal. Bioanal. Chem. 378 (2004) 1327.
[27] L. Codognoto, E. Winter, J.A.R. Paschoal, H.B. Suffredini, M.F. Cabral, S.A.S. Machado, S. Rath, Talanta 72 (2007) 427.
[28] E. Laviron, J. Electroanal. Chem. 100 (1979) 263.
[29] R.E. Dickerson, T. Takano, D. Eisenberg, O.B. Kallai, L. Samson, A. Cooper, E. Margoliash, J. Biol. Chem. 246 (1971) 1511.
[30] K. Prasad, V.A. Laxdal, M. Yu, B.L. Raney, Mol. Cell. Biochem. 154 (1996) 55.
[31] I. Borisov, A. Lobanov, A. Reshetilov, B. Kurganov, Appl. Biochem. Microbiol. 36 (2000) 215.
[32] R. Hirata, S. Matsushita, Biosci. Biotechnol. Biochem. 60 (1996) 484.
[33] M. Yin, W. Cheng, J. Agric. Food Chem. 46 (1998) 4097.